Biochimica et Biophysica Acta, 1149 (1993) 10–18

BBAMEM 75973

Electroporation in symmetric and asymmetric membranes

I. Genco, A. Gliozzi, A. Relini, M. Robello and E. Scalas

Università di Genova, Dipartimento di Fisica, Genova (Italy)

(Received 16 December 1992)

Key words: Electroporation; Electrical breakdown; Electropermeabilization

We present results of electrical measurements performed both on symmetric and asymmetric membranes in current-clamp conditions. The current–voltage characteristic curve of the membranes shows a reversible conductance transition to a higher level above a critical potential V_c. The experimental results are interpreted in the light of the electroporation theory, which allows estimates of the line tension to be made. These estimates are compared to previous experimental findings or theoretical calculations. The behaviour of symmetric membranes of different chain lengths or consisting of mixtures of short and long chains indicates a strong dependence of V_c on the chain composition and on the presence of charges on the polar head. The electroporation process is also analyzed in asymmetric bilayers consisting of a charged and an uncharged monolayer, a condition which mimics that of natural membranes. Therefore it is possible to analyze the electrical forces acting on the uncharged monolayer due to the presence of charges on the other one, under several ionic-strength conditions. It is shown that the instability arises in the uncharged monolayer, while the coupling between the two monolayers triggers the electroporation process.

Introduction

Under normal physiological conditions the electric field in a cell membrane is approximately 10^5 V/cm, which is very close to the dielectric breakdown of liquid hydrocarbons. An electroporation process occurs when a strong external electric field is applied to the membrane. This process is characterized by a very significant transient increase in conductance and permeability which is compatible with cell survival. Electroporation has a variety of applications including cell transfection for transient gene expression or for stable genome integration, insertion of proteins in living cells, encapsulation of drugs in controlled-release systems. Moreover, it seems to be the first step for electrofusion in cell membranes [1–3]. Electroporation occurs by applying electric pulses up to 10^6 V/cm with a duration ranging between microseconds and milliseconds to cell membranes in a close-contact configuration [1,2].

In spite of the widespread use of the electroporation technique in fundamental research as well as biotechnology, the detailed mechanism of the field-induced restructuring of the membranes is not completely clear. Planar lipid bilayers (BLM) have been used as model systems to investigate the electroporation process [4–6]. However, applying a steady potential difference in the order of 200–300 mV across a BLM will cause the membrane to break. Therefore, with this method, only the action of very short electric pulses lasting less than 1 ms can be investigated. The novelty of our approach is to study this phenomenon under current-clamp rather than the usual voltage-clamp conditions [6]. The current–voltage characteristic of the membrane shows a reversible conductance transition to a higher level above a critical potential, V_c. It is worth noting that this phenomenon cannot be observed under voltage-clamp conditions owing to the very short lifetime of the membrane in the new high-conductance state.

In this work we present experimental results which can be interpreted in terms of previous electroporation theories. The model predicts that the critical potential at which the transition occurs depends on the line tension of the pores and, to a lesser degree, on the surface tension of the bilayer. We performed experiments on phosphatidylcholine, phosphatidylserine and glycerol monoleate membranes. The experiments on phosphatidylcholine BLMs were performed by changing the length of the hydrophobic chains or considering mixtures of short and long chains at several molar ratios, in order to vary the intensity of the lateral interactions between molecules in the bilayer.

The electroporation process has also been analyzed in asymmetric bilayers, a condition which mimics that

Correspondence to: A. Gliozzi, Dipartimento di Fisica, Università di Genova, via Dodecaneso 33, 16146 Genova, Italy.

of natural membranes. In particular it was possible to form asymmetric membranes consisting of a charged and an uncharged monolayer and to analyze the electroporation process under several ionic strength conditions. Capacitance–voltage measurements were performed to evaluate the internal electric potential acting on the membrane [7]. These data have been compared with the theoretical values obtained using the Stern method, which is a combination of the Langmuir adsorption isotherm and the Gouy-Chapman theory for the diffuse double layer [8–10]. The experimental results indicate that once the electrostatic forces have been properly accounted for, the critical potential at which electroporation occurs is typical of a symmetric membrane formed by the lipid with the lower transition potential.

Materials and Methods

Egg phosphatidylcholine (egg PC) and cholesterol (Ch) were purchased from Calbiochem (La Jolla, CA); DilauroylPC ($(12:0)_2$PC), dipetroselinoylPC ($(18:1;\ 6cis)_2$PC), dioleoylPC ($(18:1;\ 9cis)_2$PC), diphytanoylPC (DPhPC) and phosphatidylserine (PS) were purchased from Avanti Polar Lipids (Alabaster, AL); and glycerol monoleate (GMO) was obtained from Sigma (St. Louis, MO). For the case involving asymmetric membranes, one of the monolayers was formed by egg PC/Ch mixed in the molar ratio 4:1 and the other by pure PS. KCl and $CaCl_2$ (Carlo Erba, Milan, Italy) solutions were formed using a water purification system (Milli-Q plus, Millipore Corporation, Bedford, MA). The salts were baked at 500°C for 1 h and the solutions were filtered with a Millipore filter with a diameter of 0.22 μm. Lipid bilayers were formed by hydrophobic apposition of two monolayers, obtained from lipids dissolved in n-hexane (BDH, Milan, Italy) at a concentration of 10 mg/ml.

With regard to asymmetric membranes, great care was taken to avoid contamination between the two different lipids. In this series of experiments only membranes formed after the first rise of the two monolayers were considered. After every measurement on a single membrane, the chamber was carefully cleaned and a new membrane was formed. BLMs were formed on a 160 μm diameter hole on a teflon septum separating 2 ml chambers. The electric signals were recorded by means of two Ag/AgCl electrodes. The current–voltage (I–V) characteristics were obtained under current-clamp conditions, with the membrane in a feedback network of a high-impedence (10^{13} Ω) operational amplifier (Burr Brown 3528 CM) which acts as a current–voltage converter. The I–V cycles were obtained by sending the membrane a triangular current wave, usually with a frequency of $2.5 \cdot 10^{-3}$ Hz. Once the order of magnitude of the critical potential V_c was known, the current amplitude was calculated, according to the relationship:

$$V_c > I/G_M$$

where I is the input current and G_M is the initial membrane conductance. The capacitance–voltage measurements were obtained after sending a 10 mV peak to peak and 10 kHz input sinusoidal signal through an adder circuit. By using an appropriate decoding circuit, an output signal was obtained that was proportional to the membrane capacitance. The sensitivity was on the order of 1%.

The surface tension Γ has been determined by applying a known hydrostatic pressure difference between the two half-cells of the teflon chamber and measuring the consequent change in capacitance. Further details can be found in Results.

Theoretical considerations

According to the electroporation theory [1,5,11–18] a BLM is a system in a metastable state, containing a fluctuating population of pores (or defects). The pores are considered as the nuclei of a new phase in the theory of homogeneous nucleation.

The work to form a pore of radius r is given by a balance between the energy necessary to create the edge of a pore and the energy released by the pore surface. It can be written as:

$$E(r) = 2\pi\gamma r - \pi\Gamma r^2 \tag{1}$$

where γ is the line tension and Γ is the surface energy of the bilayer.

The pore formation work also depends on the electric field (here the electroporation theory differs from the usual nucleation theory). In order to take this effect into account, Γ in Eqn. 1 must be replaced by an effective surface energy Γ_{eff}, which depends on the electric potential V applied to the bilayer given [11,12] by:

$$\Gamma_{eff} = \Gamma + aV^2 \tag{2}$$

where a is a parameter defined as

$$a = \frac{\epsilon_0}{2d}(\epsilon_w - \epsilon_l) \tag{3}$$

and d is the bilayer thickness, ϵ_0 is the dielectric permittivity of the vacuum and ϵ_w, ϵ_l are the relative permittivities, respectively of water and lipid.

The average lifetime τ of a metastable state, in the theory of homogeneous nucleation, is given [11,12] by:

$$\tau = A \exp\left(\frac{E_c}{k_B T}\right) \tag{4}$$

where k_B is the Boltzmann constant, T is the absolute temperature, and E_c is the energy barrier for pore formation, given by:

$$E_c = \frac{\pi\gamma^2}{\Gamma_{eff}} \tag{5}$$

The prefactor A in Eqn. 4 has been computed in Ref. 12 and is given by:

$$A = \frac{(k_B T)^{3/2}}{4\pi c_p S D \gamma \Gamma_{eff}^{1/2}} \tag{6}$$

where c_p is the pore concentration, S is the membrane area and D is the coefficient of pore diffusion in the space of radii.

Combining Eqns. 5 and 6 and replacing in Eqn. 4 we find the following formula for the average lifetime τ:

$$\tau = \frac{(k_B T)^{3/2}}{4\pi c_p S D \gamma \Gamma_{eff}^{1/2}} \exp\left(\frac{\pi\gamma^2}{\Gamma_{eff} k_B T}\right) \tag{7}$$

We shall use Eqn. 7 in order to estimate the line tension γ below. It is important to note that we used the simplest form of the electroporation theory when analyzing our experimental data. In particular, we have neglected the dependence of γ on the pore radius r. However, since we did not measure the average lifetime τ of the membranes, and we are interested in estimating the line tension γ for the various membranes, we consider this simpler analysis to be more than sufficient.

Results

Current–voltage characteristics recorded on symmetric membranes of egg PC/Ch and PS are reported in Figs. 1a,b. In the case of egg PC/Ch the membrane shows a conductance transition which occurs at about 270 mV and is characterized by the onset of fluctuations in the new conductance state. When the current decreases the membrane slowly recovers its initial conductance state while a new transition is observed at negative potentials at about the same absolute value. The phenomenon is also accompanied by a hysteresis effect. The critical potential at which the transition occurs depends on the nature of the lipid. Fig. 1b shows that with PS membranes the transition is not observed up to potentials as high as 400 mV. It should be pointed out that the membrane capacitance, observed before and after the transition, does not vary appreciably, which agrees with previous experimental findings [6,13,14], thus ruling out electromechanical effects [19].

The electroporation theory predicts that the critical potential V_c depends on the line tension γ and on the surface tension Γ [12]. The surface tension of PC BLMs was determined by applying a known pressure difference, ΔP, across the membrane, and measuring the capacitance C_0. Changes in C_0 values as a function of the applied pressure were used to assess the interfacial tension by means of the Laplace relationship:

$$\Delta P = \frac{4\Gamma}{R}$$

where R is the radius of curvature of the spherical cup.

TABLE I

Electric field-induced electroporation in symmetrical membranes

The critical potential V_c and the surface tension Γ are given for various lipids and lipid mixtures at different molar ratios. The line tension γ_{eff} has been calculated by using Eqn. 7 assuming $\tau = 1$ s and $\Gamma = 0.22 \cdot 10^{-3}$ J/m for all the PC membranes. * Data from Ref. 23.

Lipids	Molar ratio	V_c (mV)	Γ (10^{-3} J/m^2)	γ_{eff} (10^{-11} J/m)
Phosphatidylcholines				
(18:1; 6*cis*)$_2$PC		400±21	0.22±0.02	3.0
(18:1; 9*cis*)$_2$PC		330±23	0.22±0.02	2.5
DPh PC		390±20	0.22±0.02	2.9
Egg PC		280±30	0.22±0.02	2.1
Egg PC/Ch	4:1	270±20	0.22±0.02	2.0
Mixtures of phosphatidylcholines				
(12:0)$_2$PC/(18:1; 6*cis*)$_2$PC	1:10	380±25	0.22±0.02	2.8
(12:0)$_2$PC/(18:1; 6*cis*)$_2$PC	2:10	315±25	0.22±0.02	2.3
(12:0)$_2$PC/(18:1; 6*cis*)$_2$PC	3:10	280±25	0.22±0.02	2.0
(12:0)$_2$PC/(18:1; 6*cis*)$_2$PC	4:10	285±15	0.22±0.02	2.1
Other lipids				
PS		500±50	0.29±0.02 *	3.7
GMO		170±50	0.22±0.02 *	1.3

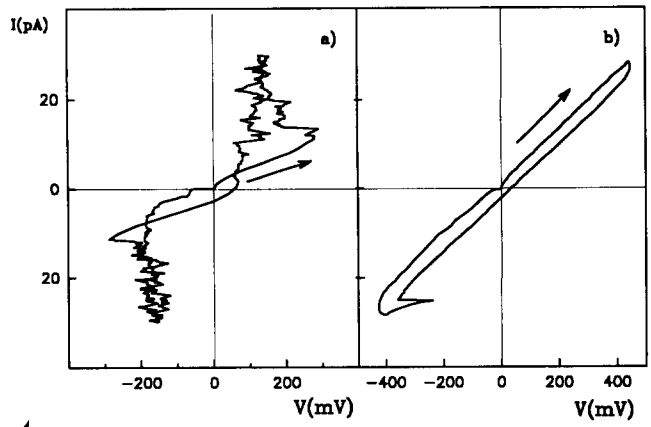

Fig. 1. Current–voltage characteristics of membranes made of (a) egg PC/Ch (molar ratio 4:1) and (b) PS. The PS membrane has a much higher transition potential value. In both cases the ionic concentration was 10^{-1} M KCl at pH 5.5.

The value obtained from the average over 20 different membranes is $\Gamma = (0.25 \pm 0.02) \cdot 10^{-3}$ J/m^2. The details of this method can be found in Ref. 20.

The V_c values of Table I are the average over at least ten different membranes. If the I–V run is repeated on the same membrane, in the second run V_c decreases by nearly 20% and then reaches an almost constant value. However, the conductance values before and after the transition are almost unaffected. We have not detected any significant variation of the above phenomena by changing the frequency from $2 \cdot 10^{-3}$–$5 \cdot 10^{-3}$ Hz.

Studies on PC BLMs in which the composition of the chains, and therefore the line tension, has been systematically varied reveal that V_c depends quite strongly on this parameter (Table I). The V_c values which were determined for PS and GMO membranes, for which the surface tension was recently evaluated, are also reported in Table I. The data shown in Table I indicate that the values of the critical potential may differ up to more than 200 mV depending on the physical properties of the lipid. This fact gave us the idea to form membranes consisting of two different monolayers with lipids characterized by very different transition potentials. In this way a transition potential very close to the smaller one would indicate that electroporation initially involves only one monolayer and that it triggers the transition on the other one. Moreover, if only one of the two monolayers is charged, the electric forces acting on the other one can be evaluated.

Asymmetric membranes were formed by PS and egg PC/Ch (4:1, molar ratio) monolayers. We found that V_c for such membranes depends on the direction of the electric field as shown in Figs. 2 and 3. When the electric field is directed towards the PC/Ch monolayer as sketched in the left-hand side of Fig. 2, V_c is higher than when it is directed towards the PS monolayer as

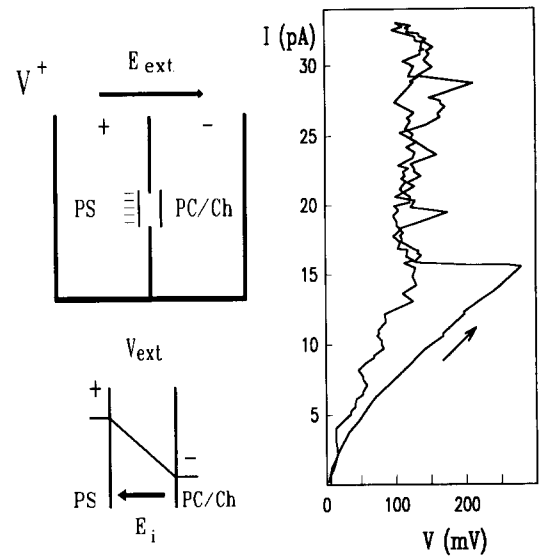

Fig. 2. A sketch of the operating configuration named V^+ is reported on the left-hand side. The potential profile, due to the external applied potential, and the direction of the internal field, E_i, are also indicated. The right-hand side shows a typical current–voltage characteristic curve of asymmetric membranes, consisting of two different monolayers of PS and egg PC/Ch (4:1 molar ratio), recorded in the V^+ configuration.

shown in Fig. 3. We shall call these two configurations V^+ and V^-, respectively. Control experiments performed by inverting the position of the monolayers indicated that this effect does not depend on the asymmetry of the experimental apparatus. The two different values of V_c might be the result of the electrostatic potential of PS (which is negatively charged) on the PC/Ch monolayer. This potential is added or subtracted to the external one, respectively, in the V^-

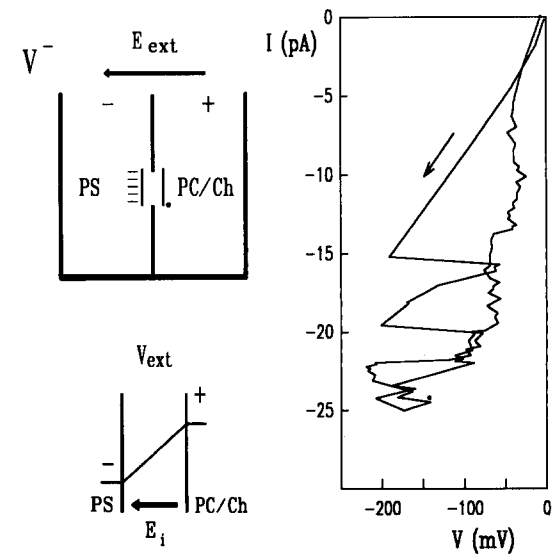

Fig. 3. A sketch of the operating V^- configuration is reported on the left hand side. The right hand side shows a typical current–voltage characteristic curve of asymmetric membranes in the V^- configuration. Other conditions as in Fig. 2.

and V^+ configuration (see Figs. 2 and 3). To test this hypothesis, measurements were performed at different ionic strengths of the bathing solutions in order to change the surface potential. The results are reported in Table II, where each value is the average over at least ten membranes. To avoid possible changes on the membrane itself, only the first transition has been considered. Inspection of Table II reveals that the difference between V^+ and V^- decreases as the ionic strength increases. This indicates that the internal electric field E_i, sketched in Figs. 2 and 3, generated by the surface charges, is one of the causes of the difference between V^+ and V^-. However, the ensuing discussion will demonstrate that besides E_i, other forces (presumably arising from the dipole orientation in the electric field) are responsible for the observed asymmetry.

A direct measurement of the internal transmembrane potential, ψ, can be obtained from capacitance changes as a function of the external potential. In fact, BLM changes in capacitance have been shown to relate to the applied transmembrane potential (see Ref. 7),

$$\frac{\Delta C}{C} = \alpha V^2 + \beta \tag{8}$$

where C is the capacitance at zero potential, α is related to the thickness elastic modulus and β is the

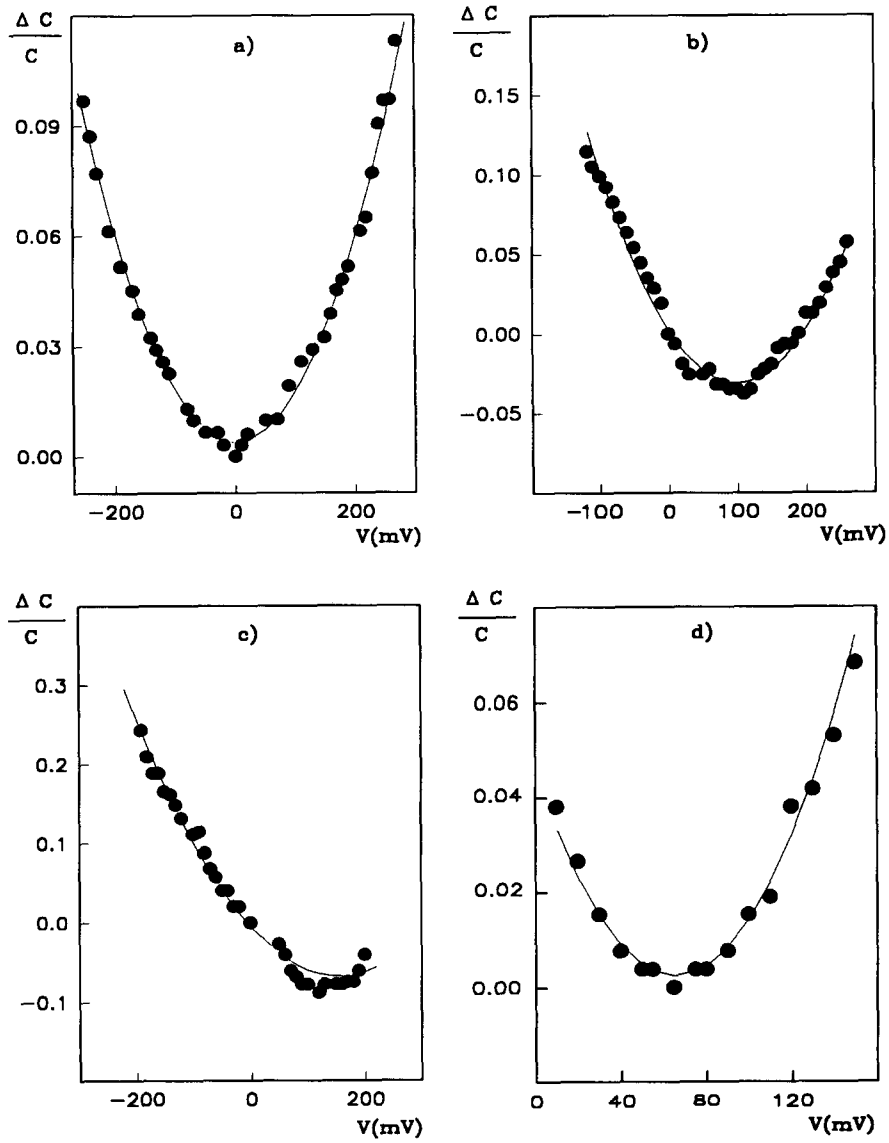

Fig. 4. Typical plots of changes in capacitance vs. the external potential: (a) symmetrical, (b–d) asymmetrical PS-egg PC/Ch membranes. Solid curves are the best fit of the experimental points with Eqns. 8 and 9. Ionic conditions and fitting parameters are:

(a) KCl 0.1 M,	$\alpha = 1.4\ V^{-2}$,	$\beta = 3.8 \cdot 10^{-3}$
(b) KCl 0.1 M,	$\alpha = 3.4\ V^{-2}$,	$\beta = -3.0 \cdot 10^{-1}$
(c) KCl 0.01 M,	$\alpha = 2.6\ V^{-2}$,	$\beta = -6.7 \cdot 10^{-2}$
(d) KCl 0.1 M, $CaCl_2$ 1 mM,	$\alpha = 10\ V^{-2}$,	$\beta = 2.5 \cdot 10^{-3}$.

TABLE II

Electric field-induced electroporation in asymmetric membranes

The transition potential of asymmetric membranes in both configurations (V^+ and V^-) is tabled for various ionic concentrations. The values of the potential, $|\psi|$, measured by using Eqn. 9 and of the surface potential $|\psi_t|$ of PS calculated by the Stern method are also reported. In the presence of $CaCl_2$ a 2:1 and a 1:1 stoichiometry have been used, respectively, in [a] and [b].

C_S (M)	V^+ (mV)	V^- (mV)	$\|\psi\|$ (mV)	$\|\psi_t\|$ (mV)
10^{-2} KCl	320±40	172±31	166±29	161
10^{-1} KCl	300±40	205±10	105±16	103
10^{-1} KCl 10^{-3} $CaCl_2$	305±11	239±16	62± 5	67 [a] 59 [b]

choice of the reference capacitance. If the membrane has an internal transmembrane potential ψ, Eqn. 8 becomes:

$$\frac{\Delta C}{C} = \alpha(V+\psi)^2+\beta \tag{9}$$

Plotting $\Delta C/C$ as a function of V, the abscissa of the minimum gives $-\psi$. Typical plots of the data for PS-egg PC/Ch BLMs in different ionic solutions are shown in Figs. 4b–d, while Fig. 4a is a control experiment on pure PS membranes. Continuous curves are the best fit of the experimental points with Eqns. 8 and 9. Each measurement was repeated with at least ten different membranes. The minimum of the parabola was determined for each membrane by using Eqns. 8 and 9 and the mean value of the minima was calculated. The values of $|\psi|$, determined by this procedure for different ionic solutions, are reported in Table II and compared with the corresponding theoretical values deduced by the Stern method, as discussed later.

In a few experiments the transition of asymmetric membranes was not observed in the usual potential range. We attributed this fact to contaminations which may have occurred among the PS and PC/Ch monolayers. To test this hypothesis we performed control experiments adding small amounts of PS to the PC/Ch monolayer and vice versa. In fact no transition was observed in the usual potential range.

Discussion

Electroporation in symmetrical and asymmetrical BLMs under current-clamp conditions was the most significant accomplishment of this work. The data presented in Results for both symmetric and asymmetric membranes will be analyzed below.

Symmetric membranes

The phenomenon we are describing indicates that an external electric field induces a sharp variation in the membrane conductance, when the potential reaches a critical value V_c. Figs. 1, 2 and 3 show that this phenomenon is accompanied by voltage fluctuations and a hysteresis effect. We can qualitatively interpret the phenomenon as due to the electric-field-induced formation of pores. The hysteresis effect and the fluctuations are consistent with the notion that the pores have a characteristic relaxation time for closing when the potential is reduced [4]. In fact, since we work in current-clamp conditions, the membrane does not rupture because of the reduction of the transmembrane voltage V, when the membrane conductance increases.

Eqn. 7 is used to estimate the line tension γ, assuming $D = 1.1 \cdot 10^{-12}$ m^2/s and $c_p = 1/h^2$ (where h is the membrane thickness) [16]. Some words of caution are necessary. First of all, we assume that the potential V_c at which the conductance transition arises, can be interpreted as the critical potential at which the irreversible breakdown would start. We do not know the exact value of the average lifetime τ at V_c, but, since the membrane does not rupture, we can say that τ is greater than τ_R, the time constant of our circuit ($\cong 40$ ms). If we solve Eqn. 7 graphically we find that the value of γ does not change considerably when τ varies in the range 10^{-2}–10^2 s. Therefore, as in Ref. 16 we assume a typical value of $\tau = 1$ s. Secondly, since we neglect the dependence of γ on the radius of the pore, properly speaking, we obtain only an effective line tension γ_{eff}. Nonetheless, the values of γ_{eff} reported in Table I agree even in terms of quantity with those obtained in other laboratories, as reported in Table III

TABLE III

Surface tension, Γ, and line tension, γ_{eff}, for various BLM systems

Data in Ref. 15 are obtained with a two-parameter fit of Eqn. 7. Data in Ref. 21 are obtained by alignment and opening of giant phosphatidylcholine vesicles by an electric field. The line tension, γ_{eff} is calculated through the relationship between γ and the curvature-elastic modulus κ: (Ref. 21; Eqn. 7). Data from Ref. 23 are obtained with optical methods using high-powered lasers. Data from Ref. 25 are obtained by the Laplace method. Finally, data from Ref. 22 come from a theoretical estimate of the lateral interactions in BLMs.

Lipids	C_S	γ_{eff} (10^{-11} J/m^2)	Γ (10^{-3} J/m)	Ref.
PE in decane.	KCl 10^{-1} M	1.58	2.7 ±0.3	15
PE in squalene	KCl 10^{-1} M	1.53	2.4 ±0.2	15
PE in squalene/LPC ($4.5 \cdot 10^{-4}$ g/l)	KCl 10^{-1} M	0.450	0.33±0.1	15
PC in decane	KCl 10^{-1} M	0.874	1.0 ±0.3	15
PC in decane/LPC ($4 \cdot 10^{-4}$ g/l)	KCl 10^{-1} M	0.352	0.2 ±0.1	15
PC cylindrical vesicles	H_2O	2.0	–	21
GMO in decane	KCl 10^{-1} M	–	0.22±0.02	23
Egg PC in dodecane	NaCl 10^{-1} M	–	0.9 ±0.1	25
Theoretical calculation	–	1.0	–	22

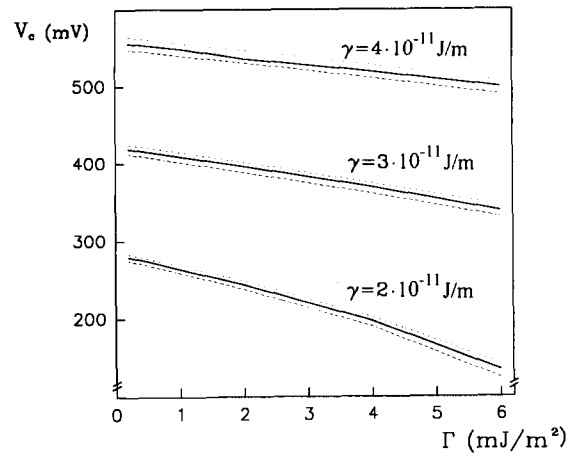

Fig. 5. The critical potential V_c has been plotted as a function of the surface tension Γ at various values of γ. The curves are obtained from Eqn. 7. The dotted and the dashed lines correspond to $\tau = 0.1$ and 10 s, respectively, while the solid line corresponds to $\tau = 1$ s.

[15]. Evaluations of γ with completely different procedures are also included [21,22].

Table I shows that the interfacial tension Γ of PC BLMs is remarkably similar to those of PS and GMO BLMs recently obtained with optical methods using high-powered lasers [23]. Earlier measurements of Γ for various lipid systems can be found in Refs. 20, 24 and 25. The trend of V_c as a function of Γ, at different values of γ, is plotted in Fig. 5. The dotted and the dashed lines correspond to $\tau = 0.1$ and 10 s, respectively, while the solid line corresponds to $\tau = 1$ s. Inspection of Fig. 5 reveals a slight dependence of V_c on Γ and a negligible dependence on τ. This fact further justifies our choice of a typical lifetime $\tau = 1$ s. The line tension γ is the edge energy of the pore walls and therefore it is expected to decrease as the chain length decreases. In fact, Table I indicates that the values of γ obtained from the lipid mixtures decrease by increasing the content of the short chains until a limiting lower value of $1.9\text{–}2.0 \cdot 10^{-11}$ J/m is reached. It has been previously shown that short chain PCs should form micelles instead of bilayers [26]. Therefore, our result could be explained by the presence of this kind of molecules, which should decrease the elastic energy of the pore edge [27]. If the percentage of short chains is further increased, then the membranes no longer form. This is probably due to lateral phase separation between the two components. In fact, as expected, we have been unable to form membranes consisting only of $(12:0)_2$PC chains. The high value of γ obtained for diphytanoylPC is an indication of the strong interaction energy between these bulky chains. The low conductivity to ions observed in all isoprenoid lipids of archaeobacteria [28] may be related to the high energy required to form aqueous pores. By contrast, the extremely small value of γ for GMO membranes is probably related to the presence of a single chain per molecule and may account for the relatively higher permeability to ions with respect to PS BLMs [24].

An important feature of Table I is the difference in the critical potential (and hence in γ) between (18:1; 9*cis*)$_2$PC and (18:1; 6*cis*)$_2$PC. This fact indicates that not only the number of double bonds, but also their position is important for the penetration of water inside the chains and thus for the formation of aqueous pores. Permeability studies of BLMs have shown that a single unsaturated bond dramatically increases the solubility of water [29]. Transient contacts between double bonds and water in DOPC bilayers have been observed in neutron lamellar diffraction data. It has been suggested that these contacts could play an important role in water permeation [30]. Indeed the formation of pores in the membrane might perhaps provide some insight for the anomalous water permeation in BLMs [31]. A theory of osmotic pressure-induced pores in phospholipid vesicles has been presented in Ref. 32 to explain the leakage of hydrophilic molecules from vesicles of egg PC and DPPC.

The charged PS membranes deserve particular attention. The data in Table I indicate that there is a relevant increase in the line tension. In these membranes there is a delicate balance between the forces of the polar heads, which include an electrostatic repulsive term and Van der Waals attractive interactions. In the case of phosphatidylethanolamine (PE) Mingins et al. [33] and Stigter et al. [34] have shown that, compared to PC headgroups repulsion, PE headgroup repulsive interactions are much weaker and this accounts for the fact that the line tension of PE is greater than that of PC (see Table III). In other words, the stronger lateral repulsion of PC makes it easier for pores to be formed. In the case of PS, if a purely repulsive charge interaction were present, one would expect a strong lateral repulsion between the headgroups, leading to a behaviour similar to that of PC membranes. It would be interesting to see whether the repulsive interaction of PS are lower than those for PC. Indeed, our results, as reported in Table I, suggest that this is the case. A change in the dipolar orientation, competing with charge repulsion, might indeed reduce the repulsive contribution. However, the energy required to form a hydrophobic pore can be higher also, due to facing of the negative charges at the pore walls.

Asymmetric membranes

The behaviour of asymmetric membranes is more intriguing. In contrast to symmetric membranes, an inspection of Table II reveals that the critical potential depends on the direction of the field. This is not surprising, since an internal potential ψ is added or subtracted to the external one, as sketched in Fig. 6. A

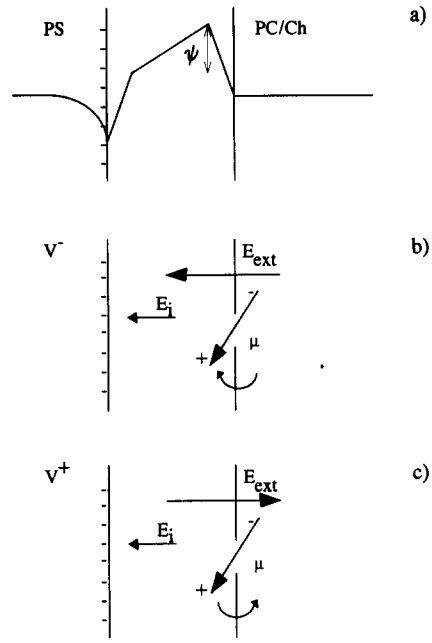

Fig. 6. (a) A sketch of the potential profile showing that an internal potential ψ stems from the presence of a charged monolayer. (b) A sketch of the external field, E_{ext}, the internal field E_i and the dipole moment μ. The external electric field, acting in the same direction as E_i, would produce a deeper penetration of the dipole into the hydrophobic core. This movement is hindered by steric interactions. (c) The external field, opposite to E_i, can decrease the out-of-plane component of the dipole moment.

determination of precise ψ values is necessary to test this simple hypothesis. The values of ψ obtained experimentally (Table II), are consistent with the theoretical values of the surface potential, which are plotted in the last column of the same Table. It is possible to calculate ψ using the Langmuir adsorption isotherm and the Gouy-Chapman theory, which yields the so-called Grahame equation [35]. If K^+ ions are the only positive ions in the solution we have:

$$\frac{\sigma}{\sigma_{max}} = \frac{1}{1 + K_K[C_K(\infty)\exp(-e\psi/k_BT)]} \tag{10}$$

$$\sigma = [8\epsilon_0\epsilon_w N_A k_B T C_K(\infty)]^{1/2} \sinh(e\psi/2k_BT) \tag{11}$$

where $K_K(\cong 0.15\ M^{-1}$ see Ref. 10) is the dissociation constant of potassium, $|\sigma_{max}|(\cong 0.25\ C/m^2)$ is the charge density in the absence of adsorption of counterions, $C_K(\infty)$ is the potassium concentration in the bulk solution, N_A is the Avogadro number and e is the electron charge.

If calcium is also present in the solution the situation is slightly different and Eqns. 10 and 11 must be replaced [35] by:

$$\frac{\sigma}{\sigma_{max}} = \{1 + K_K C_K(\infty)\exp(-e\psi/k_BT) + K_{Ca}C_{Ca}(\infty)\exp(-2e\psi/k_BT)\}^{-1} \tag{12}$$

$$\sigma = (8\epsilon_0\epsilon_w N_A k_B T)^{1/2} \sinh(e\psi/2k_BT)\{C_K(\infty) + C_{Ca}(\infty)(2+\exp(-e\psi/k_BT))\}^{1/2} \tag{13}$$

where K_{Ca} is the dissociation constant for calcium and $C_{Ca}(\infty)$ is the calcium concentration in the bulk solution. If a 2:1 stoichiometry for the PS^--Ca^{2+} binding is assumed [8], a value of 67 mV is predicted for $|\psi|$, while a 1:1 stoichiometry yields a value of 59 mV, because of the different dissociation constant [9]. It is worthwhile to emphasize the excellent agreement between the values of the internal potential obtained by using the capacitance measurements and those calculated by the Stern method.

The analysis of the experimental data indicates that $V^+ - V^- \neq 2|\psi|$, as one would expect if the asymmetry were due only to the internal field. On the other hand, control experiments (performed inverting the side of the PS monolayer) rule out the presence of an experimental bias. Therefore, we must conclude that not only the PS surface charge, but also the direction of the dipoles contributes to the V_c imbalance.

Theoretical and experimental work on the molecular origin of the internal dipole potential has shown that the water of hydration is mainly responsible of the experimentally determined positive sign of the total dipole potential [36,37].

To obtain a clearer insight about the magnitude of this effect let us consider the quantities $\varphi^+ = V^+ - |\psi|$ and $\varphi^- = V^- + |\psi|$, which correspond to the potential across the membrane once the internal field due to the charges is taken into account. In particular, if we plot φ^+ and φ^- vs. $|\psi|$, the surface potential, we obtain the graph shown in Fig. 7. The two straight lines intersect at $|\psi| \cong 0$ where $\varphi^+ \cong \varphi^- \cong 270$ mV, a value which corresponds to the critical potential of a symmetric egg PC/Ch membrane. This finding is an addi-

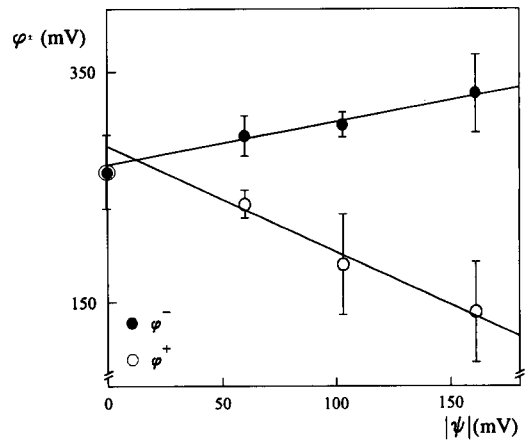

Fig. 7. A plot of the effective critical potential φ (corrected for the internal potential) vs. the surface potential $|\psi|$. $\varphi^+ = V^+ - |\psi|$; $\varphi^- = V^- + |\psi|$. Notice that when $|\psi| \to 0$, $\varphi^+ \cong \varphi^- \cong 270$ mV, a value which corresponds to the critical potential for symmetric egg PC/Ch membranes.

tional suggestion that the asymmetry in the transition potential is related to the presence of charges. Moreover, it also indicates that the transition is initiated by the egg PC/Ch monolayer, an entirely new result showing that, although the first step of the instability initates only in one layer, the coupling between the two monolayers triggers the entire electroporation process.

Fig. 7 shows that in the φ^- case there is only a slight increase in the transition potential as the charge density is increased. This may indicate that the contribution due to the dipole orientation in the PC/Ch monolayer is rather small, since the dipoles are already oriented in the direction of the internal field, an orientation which makes the system more stable. Moreover, steric repulsions prevent the dipoles from rotating, as sketched in Fig. 6b. On the other hand, in the φ^+ case the dipoles tend to assume a configuration which is different from the equilibrium arrangement, since the normal component of the dipole moment tends to decrease, as sketched in Fig. 6c. Noting that the dipole moment on the membrane plane increases, we can argue that a stronger lateral repulsion occurs, leading to a smaller critical potential.

As a direct consequence of this analysis we can speculate that even in symmetric membranes the directionality of an external field induces asymmetry in the orientation of the dipoles, which unbalances the critical potential for the formation of aqueous pores in the two monolayers of the membrane.

Acknowledgements

We thank Miss G. Accardo for help in portions of the experimental work. This work has been supported by Ministero dell'Università e della Ricerca Scientifica e Tecnologica (MURST) 40% and 60% grants and by Progetto Finalizzato Chimica Fine CNR.

References

1 Neumann, E., Sowers, A.E. and Jordan, C.A., eds. (1989) Electroporation and Electrofusion in Cell Biology, Plenum Press, New York.
2 Tsong, T.Y. (1991) Biophys. J. 60, 297–306.
3 Zimmermann, U. (1982) Biochim. Biophys. Acta 694, 227–277.
4 Benz, R. and Zimmermann, U. (1981) Biochim. Biophys. Acta 640, 169–178.
5 Glaser, R.W., Leikin, S.L., Chernomordik, L.V., Pastuschenko, V.F. and Sokirko, A.I. (1988) Biochim. Biophys. Acta 940, 275–287.
6 Robello, M. and Gliozzi, A. (1989) Biochim. Biophys. Acta 982, 173–176.
7 Usai, C., Marchetti, C., Gambale, F., Robello, M. and Gorio, A. (1983) FEBS Lett. 153, 315–319.
8 Ohki, S. and Kurland, R. (1981) Biochim. Biophys. Acta 645, 170–176.
9 McLaughlin, S., Mulrine, N., Gresalfi, T., Vaio, G. and McLaughlin, A. (1981) J. Gen. Physiol. 77, 445–473.
10 Eisenberg, M., Gresalfi, T., Riccio, T. and McLaughlin, S. (1979) Biochemistry 18, 5213–5223.
11 Abidor, I.G., Arakelyan, V.B., Chernomordik, L.V., Chizmadzhev, Yu.A., Pastushenko, V.F. and Tarasevich, M.R. (1979) Bioelectrochem. Bioenerg. 6, 37–52.
12 Pastushenko, V.F., Chizmadzhev, Yu.A. and Arakelyan, V.B. (1979) Bioelectrochem. Bioenerg. 6, 53–62.
13 Chernomordik, L.V. and Abidor, I.G. (1980) Bioelectr. Bioenerg. 7, 617–623.
14 Chernomordik, L.V., Sukharev, S.I., Abidor, I.G. and Chizmadzhev, Yu.A. (1982) Bioelectrochem. Bioenerg. 9, 149–155.
15 Pastushenko, V.F., Chernomordik, L.V. and Chizmadzhev, Yu.A. (1985) Biol. Membr. 2, 813–819.
16 Powell, K.T. and Weaver, J.C. (1986) Bioelectrochem. Bioenerg. 15, 211–227.
17 Weaver, J.C., Mintzer, R.A., Ling, H. and Sloan, S.R. (1986) Bioelectrochem. Bioenerg. 15, 229–241.
18 Powell, K.T., Derrick, E.G. and Weaver, J.C. (1986) Bioelectrochem. Bioenerg. 15, 243–255.
19 Crowley, J.M. (1973) Biophys. J. 13, 711–724.
20 Moran, A. and Ilani, A. (1970) Chem. Phys. Lipids 4, 169–175.
21 Harbich, W. and Helfrich, W. (1979) Z. Naturforsch. 34A, 1063–1065.
22 Litster, J.D. (1975) Phys. Lett. 53A, 193–194.
23 Picard, G., Denicourt, N. and Fendler, J.H. (1991) J. Phys. Chem. 95, 3705–3715.
24 Tien, H.T. (1974) Bilayer Lipid Membranes (BLM), Theory and Practice, Marcel Dekker, New York.
25 Tien, H.T. and Diana, A.L. (1967) Nature 215, 1199–1200.
26 Israelachvili, J.N., Mitchell, D.J. and Ninham, B.W. (1977) Biochim. Biophys. Acta 470, 185–201.
27 Chernomordik, L.V., Kozlov, M.M., Melikyan, G.B., Abidor, I.G., Markin, V.S. and Chizmadzhev, Yu.A. (1985) Biochim. Biophys. Acta 812, 643–655.
28 Gliozzi, A., Paoli, G., Rolandi, R., De Rosa, M. and Gambacorta, A. (1982) Bioelectrochem. Bioenerg. 9, 591–601.
29 Petersen, D.C. (1983) Biochim. Biophys. Acta 734, 201–209.
30 Wiener, M.C. and White, S.H. (1992) Biophys. J. 61, 434–477.
31 Finkelstein, A. (1987) Water Movement Through Lipid Bilayers, Pores, and Plasma Membranes – Theory and Reality, Wiley, New York.
32 Taupin, C., Dvolaitzky, M. and Sauterey, C. (1975) Biochemistry 21, 4771–4775.
33 Mingins, J., Stigter, D. and Dill, K.A. (1992) Biophys. J. 61, 1603–1615.
34 Stigter, D., Mingins, J. and Dill, K.A. (1992) Biophys. J. 61, 1616–1629.
35 Israelachvili, J.N. (1991) Intermolecular and Surface Forces, Academic Press, London.
36 Zheng, C. and Vanderkooi, G. (1992) Biophys. J. 63, 935–941.
37 Gawrisch, K., Ruston, D., Zimmerberg, J., Parsegian, V.A., Rand, R.P. and Fuller, N. (1992) Biophys. J. 61, 1213–1223.